

Ammonia sensing by hydrochloric acid doped poly(*m*-aminophenol)–silver nanocomposite

Pradip Kar · Narayan C. Pradhan ·
Basudam Adhikari

Received: 3 October 2010 / Accepted: 6 December 2010 / Published online: 21 December 2010
© Springer Science+Business Media, LLC 2010

Abstract Processable poly(*m*-aminophenol) (PmAP) was synthesized using ammonium persulfate oxidant in 0.6 M sodium hydroxide solution at room temperature. Then, *in situ* PmAP–silver nanocomposite film was obtained by casting PmAP film from dimethyl sulfoxide with silver hydroxide ammonia mixture at 140 °C. The nanocomposite film was doped with hydrochloric acid (HCl) by general solution doping technique. The undoped and HCl-doped films were characterized by ultraviolet visible spectroscopy, Fourier transformed Infrared spectroscopy, transmittance electron microscopy (TEM), scanning electron microscopy (SEM) and X-ray diffraction analysis. Spectroscopic characterizations confirmed that the PmAP was doped by silver nanoparticles and it was further doped by HCl used. So, the synthesized PmAP–silver nanocomposite showed a conductivity of 1.01×10^{-6} S/cm, which was increased to 3.27×10^{-4} S/cm after HCl doping. The well dispersed silver nanoparticles with average size 130–150 nm was observed by SEM and TEM analysis. Unlike conventional ammonia sensor here, the resistivity of the nanocomposite film was decreased on exposure to ammonia gas and the sensing properties of the HCl-doped nanocomposite films were also reproducible. It can be

seen that the % response of doped nanocomposite was unchanged while, the response time was decreased with increasing ammonia vapor concentrations in air. The ammonia-sensing characteristics of the HCl-doped nanocomposite film was explained on the basis of a proposed mechanism.

Introduction

Polyaniline and its derivatives as promising conducting polymers have received overwhelming interests in recent years. This is due to its easy synthesizability, good environmental and chemical stability and wide applicability. Polyaniline and its derivatives are widely applied in various fields such as sensors, actuators and electric devices [1, 2]. The advantages of these polymers as sensor materials are high sensitivity, reversible response and short response time when compared to other conducting polymers. With this addition, nanocomposites of conducting polymers with fillers such as metallic, ceramic and carbon black particles [3–10] generally improve the electrical properties and the sensor performance. Thus, conducting polyaniline and its derivatives have been employed as effective sensor matrices for the preparation of nanocomposites with metals or metal compounds [3–5]. In literature, composites of nano-scale metal clusters with the polyaniline and its derivatives are extensively documented as highly sensitive and selective sensor materials [11–14]. However, the synthesis of metal nanoparticles having desired shape and size with uniform distribution in the polymer matrices remains still highly challenging.

High concentrations of ammonia are easily detected by human nose, as the gas has a very pungent odor. But the detection of ammonia at low concentrations is difficult as

P. Kar (✉)
Department of Polymer Engineering,
Birla Institute of Technology, Mesra, Ranchi 835215, India
e-mail: pkar@bitmesra.ac.in; pradipkgp@gmail.com

N. C. Pradhan
Chemical Engineering Department, Indian Institute
of Technology, Kharagpur 721302, India

B. Adhikari
Materials Science Centre, Indian Institute of Technology,
Kharagpur 721302, India

the human nose fails to sense [15]. The important area of applications for ammonia gas sensors are: high volume control of combustibles in the chemical industry, exhaust gas sensors for emission control in automotive applications or monitoring of dairy products for the food industry [15]. Generally, polyaniline and its derivatives doped with protonic acids are the first choice for ammonia sensing over the others [16–22]. In spite of having various advantages, some fundamental problems for polyaniline and its derivatives as ammonia sensor are unsatisfactory low responses with high response time and irreversible recovery of the sensing film properties. The response time for ammonia sensing by polyaniline is reported around 4 min and the response of the polyaniline film generally depends on the concentration of ammonia with very weak irreversibility [23]. Chabukswar et al. [24] reported good reversible response for ammonia at very low concentration with moderate response time using polyacrylic acid–polyaniline blend, but recovery time for the sensor is high. The PANI film doped with nickel containing anions showed some weak sensitivity to ammonia gas [25].

In literature, application of poly(*m*-aminophenol) (PmAP) is reported as electrocatalytic sensors [26], but there is no report on the use of PmAP as gas sensing material. The reason might be due to very poor processability and conductivity of the polymer. However, we have already reported better processable [27] PmAP having free –OH groups. In this communication, we want to report the *in situ* synthesis of PmAP–silver nanocomposite film by thermal decomposition. Then the film is doped with aqueous hydrochloric acid by solution doping and the ammonia-sensing characteristic of the film was studied at room temperature (30 °C) and room humidity (65% RH). The ammonia vapor sensing characteristics of the film was recorded in terms of decrease in the resistivity for various vapor concentration in air–ammonia vapor mixture.

Experimental

Materials

The crystalline synthesis grade *m*-aminophenol was used as received from Loba Chemicals, India. The sodium hydroxide pellets (Quest Chemicals, India), crystalline silver nitrate (Merck, India), hydrochloric acid (S.D. Fine Chem., India), Ammonia solution (Merck, India), organic solvents, e.g., dimethylsulfoxide (DMSO) (Merck, India), acetone (Merck, India) were used without further purification. Deionised (DI) water was used for all purposes.

Synthesis of PmAP

The poly(*m*-aminophenol) was synthesized in aqueous sodium hydroxide medium using ammonium persulfate oxidant following the optimized conditions reported earlier [27]. Meta-aminophenol (0.030 mM) was dissolved in 50 mL of 0.6 M aqueous sodium hydroxide in a two-necked round-bottomed flask (RB) followed by the addition of ammonium persulfate (APS) (0.045 mM) solution in water (25 mL) in one lot to this monomer solution. The reaction was started at room temperature (30 °C) and continued up to 4–5 h in a stirring condition. A dark-brown precipitate of PmAP was obtained. The precipitate was filtered and washed 4–5 times with 4 M HCl to remove unreacted monomers or oligomers. The precipitate was further washed with DI water several times till filtrate became neutral. The deep brown colored product was dried at 60–70 °C in a vacuum oven for about 12 h.

Film casting of PmAP–silver nanocomposite

About 0.7–0.8 g PmAP was dissolved in 10–15 mL of DMSO. 5% (w/w) of silver nitrate was dissolved in excess ammonia solution (3–5 mL) and this solution was mixed with the DMSO solution of the PmAP in a beaker. The calculated percentage of silver nanoparticles was 3.2% for the reaction mixture. The beaker containing the above mixture was placed on an ultrasonic bath for 1 h continuous stirring. Then the mixture was poured on a Petri dish of diameter 10 cm and placed inside an oven maintained at 140 °C for 7–8 h. After complete evaporation of the solvent, a blackish film was formed. Next the polymer film was dipped 4–5 times alternately in deionized water and acetone to remove trapped DMSO. After proper drying, this film was then used for characterizations.

Preparation of PmAP–silver nanocomposite powder

Silver nitrate and PmAP were mixed as described in the above section. Here, only excess DMSO (20–25 mL) was used so that after 7–8 h at 140 °C the polymer film was not obtained due to the presence of excess DMSO. The dense DMSO suspension of the PmAP–silver nanocomposite was taken out from the oven and was mixed with excess acetone. Then PmAP–silver nanocomposite was precipitated out and this precipitate was filtered and properly washed with acetone and DI water. The powder PmAP–silver nanocomposite was used for the characterization purpose.

Hydrochloric acid (HCl) doping of PmAP–silver nanocomposite

The PmAP–silver nanocomposite film or powder was doped with hydrochloric acid by solution doping technique. A part of the nanocomposite film or powder was dipped in 3–4 M hydrochloric acid. After 8 h the film was taken out and the powder was filtered out. The doped nanocomposite film or powder was washed with acetone 2–3 times. The doped film was dried in a vacuum desiccator for a day.

Characterizations

DC-conductivity measurement

A standard four-point probe system [28] with a Keithley 2400 programmable current source and Keithley 2000 digital multimeter was used to measure the electrical conductivity of the sample films having thickness within 0.7–0.8 mm. Conducting silver paste adhesive was used to make a contact of copper wire with the film keeping a 1 mm gap between the probes.

SEM and EDX analysis

For the surface morphology study, the SEM images of the undoped and hydrochloric acid doped nanocomposite films were observed in a SEM instrument (VEGA TESCAN). EDX (Inca Energy, Oxford Instruments Microanalysis Ltd.) was carried out to determine the surface composition of nanocomposites.

TEM analysis

The nanoparticles size and distribution of undoped and HCl-doped PmAP–silver nanocomposite films were studied with a transmission electron microscopy (TEM, Jeol JSM 2500). TEM images were taken by placing a drop of the powder nanocomposite in acetone suspension onto a carbon coated copper grid.

UV–VIS spectra

The UV–VIS spectra of PmAP, undoped and hydrochloric acid doped PmAP–silver nanocomposite films (thickness within 0.7–0.8 mm) were recorded in reflection mode using a Mikropack UV–VIS-NIR, DH 2000 spectrometer. The UV–VIS spectrum of the ammonia exposed hydrochloric acid doped PmAP–silver nanocomposite film was obtained by subjecting the film to ammonia chamber (100 ppm) for 1 h.

FTIR spectra

The PmAP, undoped and hydrochloric acid doped PmAP–silver nanocomposites were characterized by Thermo Nicllet Nexus 870 Spectrophotometer. The spectrum of the dry sample powder in KBr pellet was recorded from 400 to 4,000 cm^{-1} .

XRD analysis

XRD of PmAP, undoped and hydrochloric acid doped PmAP–silver nanocomposite films were done with a Rigaku Ultima-III X-ray instrument using Cu K_α ($\lambda = 1.542 \text{ \AA}$). The 2θ angle range was from 10 to 90°.

Ammonia vapor sensing study

The doped nanocomposite film specimen (1 cm × 1 cm) was attached on a Bakelite sheet and then two contacts were made on the specimen by copper wires and silver paste with 2 mm distance between the probes. Then the whole arrangement was placed inside the measuring cell having one inlet for ammonia and another outlet for the same. In sensor setup [29], the ammonia–air mixture was taken from the headspace of a bottle containing ammonia solution. The ammonia concentration in the mixture was estimated by trapping a known volume in ice-cold dilute hydrochloric solution that was titrated with standard sodium hydroxide before and after ammonia trapping. Constant current was passed through the nanocomposite film by a constant current source, and a multimeter was used to measure the voltage at specific time interval. In a 10 μA constant current and 2.1 V voltage, the resistivities were measured using a multimeter (Keithley 2400) at a particular time interval. Some known volumes of the ammonia gas were introduced (concentration determined to be at 100, 250, 500, 1,000 ppm) and the changes of resistivity were recorded at every 30 s allowing the reading to stabilize. After some time when the response (R/R_0) became saturated the ammonia gas flow was stopped and air was passed to allow the sensor element to recover to the original state. Here, R_0 is the resistivity of hydrochloric acid doped PmAP–silver nanocomposite film in air and R is that of the film in presence of ammonia. The response time was measured as the time between the injection of the ammonia gas and the nanocomposite film sensor to the just beginning of response saturation. The recovery time is the time in between the saturation response to the initial value in presence of air. The sensitivity (S) of the sensor is expressed as the ratio of the change of resistivity (ΔR) due to exposure to the test gas to the resistivity (R_0) of the sample in the air [30, 31].

$$S = \frac{\Delta R}{R_0} \times 100\% \quad (1)$$

where, ΔR is the resistivity difference between R and R_0 .

Results and discussion

Doping and conductivity

The general solution doping condition is used for the doping of PmAP–silver nanocomposite by hydrochloric acid [32–35] just like polyaniline and its derivatives. Doping of PmAP with hydrochloric acid is not possible as it is not able to break the hydrogen bonding within the polymer chain [27, 36]. The silver nanoparticles are trapped by the free –OH groups of the polymer by the breaking the hydrogen bonding with the nearest >N-group [37]. The dopant hydrochloric acid now can easily protonate the >N-groups of PmAP–silver nanocomposite having weak or no hydrogen bonding with –OH groups due to incorporation of silver nanoparticles [37]. Here, silver nanoparticles act also as a dopant for PmAP having conductivity $<10^{-12}$ S/cm and thus the PmAP–silver nanocomposite shows electrical conductivity 1.01×10^{-6} S/cm [37]. The conductivity of hydrochloric acid doped PmAP film is increased to 3.27×10^{-4} S/cm due to the further doping by the hydrochloric acid.

Morphological analysis

Figure 1 shows the SEM micrographs and Fig. 2 shows the dark field TEM images of undoped and hydrochloric acid doped PmAP–silver nanocomposites. The SEM micrographs of both the nanocomposites exhibit a uniform dispersion of the silver nanoclusters in the PmAP matrix with a minimal aggregation effects (Fig. 1). The particles clusters are of spherical nature and seem to be nanosized. The TEM images of both the nanocomposites (Fig. 2) bring additional information about the size and dispersion of nanoclusters within the polymer matrix. Silver nanoclusters appeared as dark-white spots, which are clearly observed in the dark PmAP matrix background (Fig. 2). The average size of these clusters is determined as 130–150 nm ranging from 80–300 nm in both the cases. Comparing the SEM and TEM images of undoped and doped nanocomposite, it can be deduced from the images that the silver nanoclusters remain unaffected after hydrochloric acid doping in the polymer matrix.

EDX analysis

EDX analysis was performed to analyze the elements present in the surface of the samples. The EDX spectra of

undoped and hydrochloric acid doped PmAP–silver nanocomposites are shown in Fig. 3. In the undoped nanocomposite, some sulfur is present since peak for sulfur in the EDX spectra (Fig. 3a) is observed. This is due to the incorporation of some bisulfate anions (HSO_4^-), formed from the oxidant APS, in the polymer chain [29, 38]. In the EDX spectra of hydrochloric acid doped nanocomposite this above peak disappeared probably due to the replacement of bisulfate by the chloride ion (Fig. 3b). From the EDX spectral analysis, it is found that the atomic percentage of silver:chlorine was 1:2.2. This atomic ratio confirmed that, doping occurred only in those >N-sites that are free from hydrogen bonding and one silver atom resulting in two active sites for doping. This is due to the fact that, silver nanoparticles which exist as silver ion during the start of the synthesis are able to break or weaken the nearer hydrogen bonds in the PmAP chain by complex formation with the nearest electron donating groups like >N- or –OH [37]. The above explanation is also established indirectly from the fact that in normal condition doping of PmAP by hydrochloric acid is not possible [36].

UV–VIS spectral analysis

The UV–VIS spectra of the films are shown in Fig. 4. As PmAP is synthesized in basic medium the reduced form [29, 36] or very little doped form is obtained and thus PmAP film shows only one strong absorption maximum at around 300 nm for $\pi-\pi^*$ transition of conjugated aromatic system (Fig. 4a). After silver nanoparticles incorporation two broad absorption maxima appear at 500 and 750 nm (Fig. 4b). The absorption maximum at 500 nm is the combination of characteristic band of silver nanoparticles and the transitions involving the delocalized highest occupied molecular orbital (HOMO) to a virtual orbital which is localized in the quinone-dimine portion of the polymer (Fig. 4b–d), as described for polyaniline [39]. The other newly obtained absorption maxima at 750 nm (Fig. 4b, c, d), which is absent in UV–VIS of PmAP is due to the polaron transition of nanocomposite [37] due to strong doping effect of silver nanoparticle. For PmAP–silver nanocomposite doped with hydrochloric acid, three bands are appeared at 500, 630 nm (weak) and 740 nm (Fig. 4c). Here, the absorption maxima at 500 and 750 nm can be assigned for the same $\pi-\pi^*$ transition and polaron transition like the undoped nanocomposite sample. The polaron, which is formed due to the protonation by the hydrochloric acid, gives absorption maximum at 630 nm (Fig. 4c) like sulfuric acid doped PmAP [36]. The UV–VIS spectrum remains unchanged after ammonia absorption for hydrochloric acid doped PmAP–silver nanocomposite except the peaks are broadening (Fig. 4d), which indicates

Fig. 1 SEM images of **a** undoped and **b** HCl-doped PmAP–silver nanocomposite free standing films

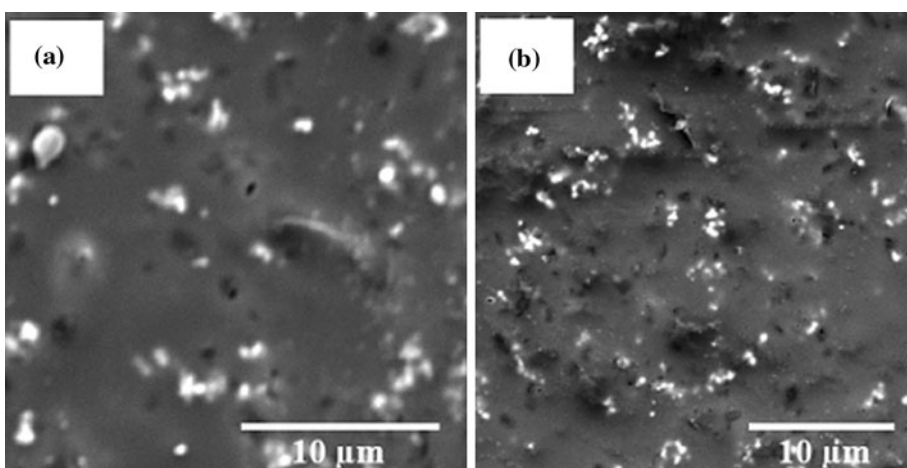


Fig. 2 Dark field TEM images (30 KX magnification) of **a** undoped and **b** HCl-doped PmAP–silver nanocomposite

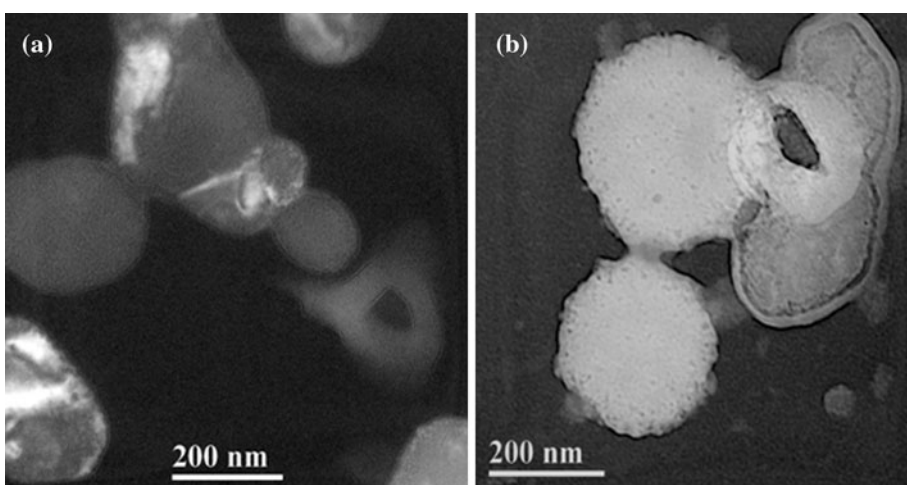
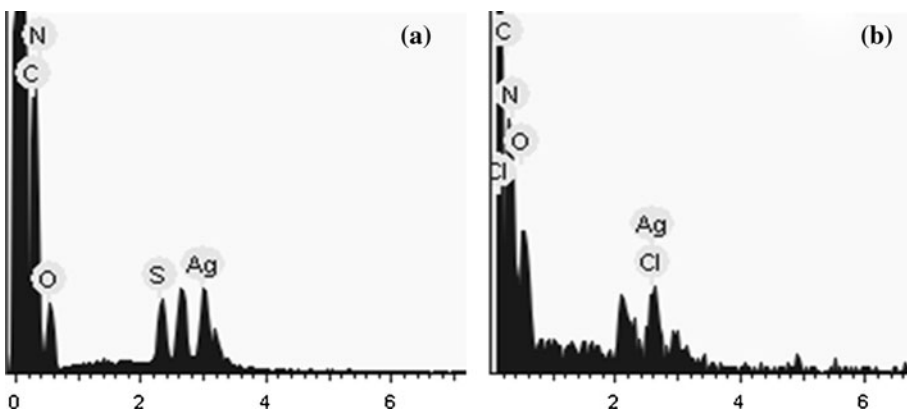


Fig. 3 EDAX spectra of **a** undoped and **b** HCl-doped PmAP–silver nanocomposite films



better delocalization of the π -electrons throughout the polymer chain after ammonia absorption.

FTIR spectral analysis

The FTIR data of the PmAP, undoped and hydrochloric acid doped PmAP–silver nanocomposite are shown in Table 1, as obtained from Fig. 5. A broad band appears for

all samples in the region 3,690 to 1,833 cm^{-1} (Table 1), which is due to the stretching of aromatic C–H, hydrogen bonded –OH, and –NH– groups (Fig. 5). The basic pattern of the bands in all FTIR spectra is almost the same except an extra band at around 2,240 cm^{-1} (Table 1) for undoped and doped PmAP–silver nanocomposite (Fig. 5). This is probably due to some strong interaction of silver nanoparticles with C=N, which achieves some triple bond

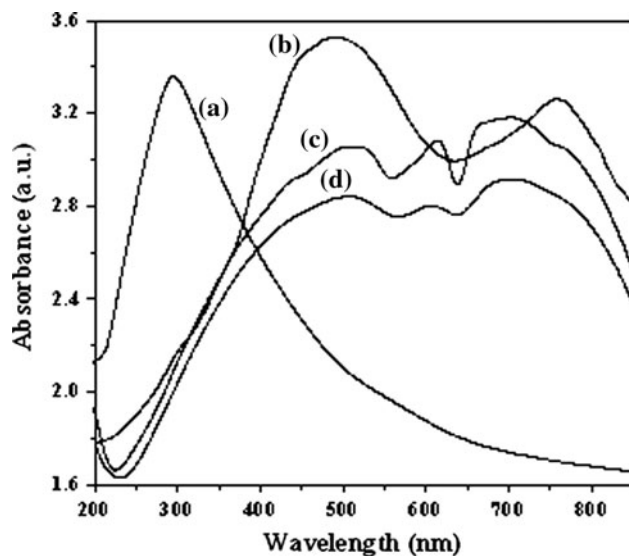


Fig. 4 UV–VIS spectra of (a) PmAP (b) undoped PmAP–silver nanocomposite (c) HCl-doped PmAP–silver nanocomposite and (d) ammonia absorbed HCl-doped PmAP–silver nanocomposite films

character and gives the characteristic stretching band at $2,240\text{ cm}^{-1}$ [40]. The band may also arise due to the characteristic absorption by cyano (CNO) group, which is obtained from the C=N group by high-temperature oxidation [41]. So, it can be deduced from the FTIR spectra that the silver nanoparticles strongly interact with the $>\text{N}-$ groups within the polymer chain which may cause the breaking of the hydrogen bond between $-\text{OH}$ and $-\text{NH}-$ groups. However, in the hydrochloric acid doped PmAP–silver nanocomposite, the intensity of the band is decreased. This is because of the protonation of aromatic C=O groups to C–OH group by the hydrochloric acid. The positions of all the FTIR bands in undoped and hydrochloric acid doped PmAP–silver nanocomposite have a little red shift when compared with FTIR bands of PmAP (Table 1). This is the evidence of doping of PmAP–silver nanocomposite by hydrochloric acid.

Table 1 FTIR spectral analysis data of the samples

PmAP	PmAP–silver nanocomposite	HCl-doped PmAP–silver nanocomposite	Responding groups	Mode of vibration
3,426 (broad)	3,424	3,389	$-\text{OH}$ (hydrogen bonded)	Stretching
3,240 (broad)	3,239 (broad)	3,169 (broad)	$-\text{NH}-$ (aromatic ring)	Stretching
2,923 (broad)	2,921 (broad)	2,920 (broad)	C–H (aromatic)	Stretching
–	2,240	2,240	CNO and $\text{C}\equiv\text{N}$	Stretching
1,625	1,620	1,620	$-\text{NH}$	Bending
1,230	1,170	1,175	$\text{C}=\text{N}$	Stretching
			C–O (alcohol)	Stretching
			C–N (polymer chain)	Stretching
1,050	1,027	1,110	C–O (C–O–H bond)	Bending
900–600 (847)	900–600 (838)	900–600 (844)	C–H (aromatic)	Bending

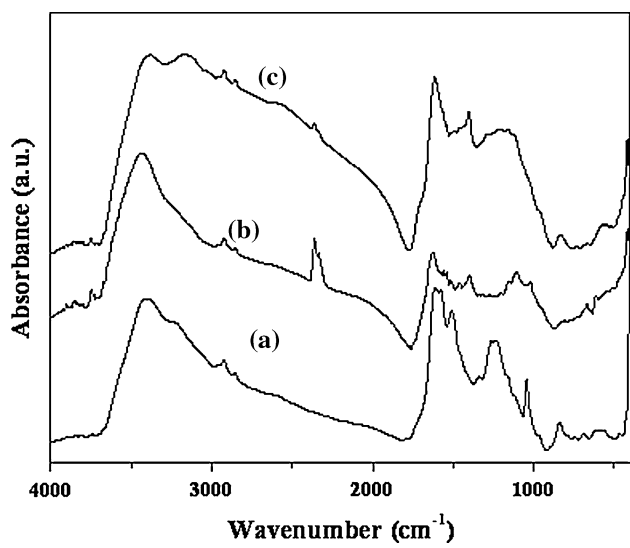


Fig. 5 FTIR spectra of (a) PmAP and (b) undoped PmAP–silver nanocomposite and (c) HCl-doped PmAP–silver nanocomposite

XRD analysis

X-ray diffraction patterns of PmAP, undoped and hydrochloric acid doped PmAP–silver nanocomposite films are shown in Fig. 6. The X-ray pattern of PmAP exhibits amorphous patterns with a broad scattering at 2θ values between 20 and 35°, while in case of undoped and doped PmAP–silver nanocomposite films some sharp peaks are obtained at 2θ values ~ 37.40 , 46.20 , 64.40 and 77.10 degree (Fig. 6b). These imply the presence of a rigid and ordered region inside the PmAP due to the silver nanoparticles crystallinity. In the XRD patterns of undoped and doped PmAP–silver nanocomposite films, the sharp peaks are detected at $2\theta = \sim 37.40$, 46.20 , 64.40 and 77.10° representing the crystal planes of (111), (200), (220) and (311) of face-centered-cubic for silver (Fig. 6c). The XRD patterns of doped and undoped PmAP–silver nanocomposite films are exactly same and so, it confirms the

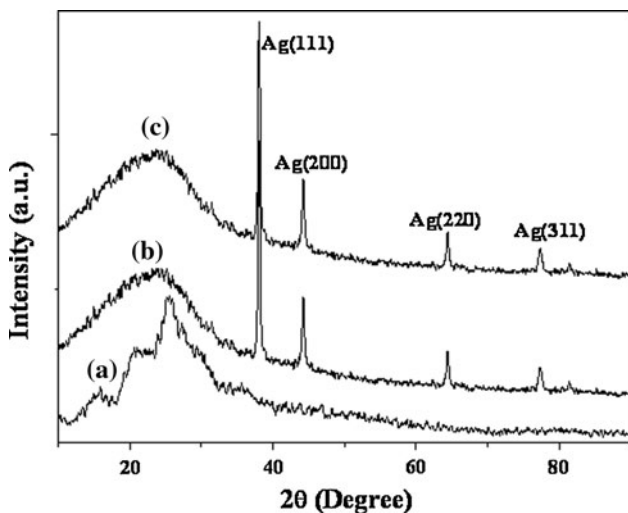


Fig. 6 XRD spectra of (a) PmAP, (b) undoped and (c) HCl-doped PmAP–silver nanocomposite films

presence of zero-valent silver nanoparticles inside the polymer matrix before and after hydrochloric acid doping.

Sensing mechanism and kinetic study for ammonia vapor sensing

During ammonia sensing, resistivity of polymer decreases and becomes constant at saturation, followed by increase in resistivity during ammonia desorption by air purge (Fig. 7). The film has no response for blank situation, i.e., without ammonia vapor (taking water only). However, at the RH as we are using the continuous flow process having outlet then the humidity inside the chamber will always be maintained

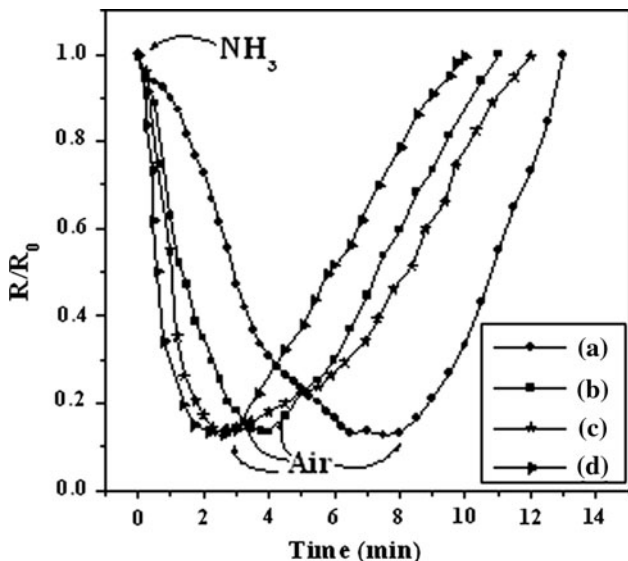
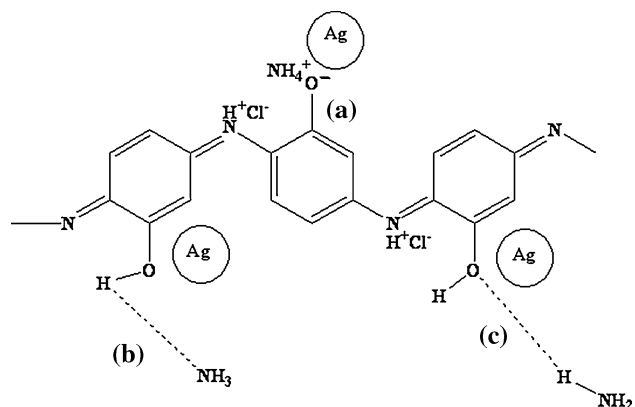


Fig. 7 Ammonia vapor sensing characteristics of HCl-doped PmAP–silver nanocomposite at varying concentration in air mixture, viz. (a) 100 (b) 250 (c) 500 (d) 1,000 ppm

as 65%. In that situation, we can conclude that water vapor does not interfere with the ammonia-sensing properties of the nanocomposite film. The increase in resistivity was reported earlier during the ammonia vapor sensing by the protonic acid doped polyaniline and its derivatives. This is because of the weak doping effect of NH_4^+ , which is obtained due to combination of H^+ dopant and NH_3 gas [29]. But here, the opposite effect is observed, which can be explained from the proposed mechanism as shown in Scheme 1. The mechanism is same as we have described for aliphatic alcohol vapor sensing using sulfuric acid doped PmAP [31]. The $-\text{OH}$ groups free form hydrogen bonding in the doped nanocomposite get hydrogen bonded or weakly protonated to NH_3 (Scheme 1). The interactions of ammonia vapor with the nanocomposite by three possible pathways are shown in Scheme 1. Due to these interactions, a weak electron donation effect occurs through the $-\text{OH}$ group to the polymer chain and ultimately the electron flow throughout the polymer chain increases. However, perhaps some ionic conduction is also possible during the ammonia sensing due to the formation of the $-\text{O}-\text{NH}_4^+$ species. Here, the sensing of ammonia vapor by undoped nanocomposite film following the same mechanism is also possible, but since the resistivity is very less the change of resistivity is unpredictable. Like polyaniline and its derivatives the reaction of ammonia molecule to $=\text{NH}_4^+$ -groups is difficult due to the steric hindrance of silver nanoparticles and free $-\text{OH}$ groups. Here, the role of silver nanoparticle is to break the hydrogen bonding and $-\text{OH}$ groups become exposed to ammonia vapors. The other role of silver nanoparticles is the enhancement of interactions between the analyte ammonia and the functional groups of the polymer by catalytic surface activity of silver nanoparticles [42, 43]. The response obtained from the dynamic response curves are plotted as a function of vapor concentrations for ammonia vapor in air (Fig. 8). It



Scheme 1 Interactions of ammonia vapor with the hydrochloric acid doped PmAP–silver nanocomposite by three possible pathways (a), (b) and (c)

can be seen that the responses of hydrochloric acid doped PmAP–silver nanocomposite shows linear relationship with increasing ammonia vapor concentrations in air (Fig. 8). The % sensitivity and response time for different concentrations of ammonia vapor in air are shown in Table 2. The average relative response is 86.75% with a standard deviation of ± 2.9 which is added as error bar in Fig. 8. Only the response times (Table 2) decrease as the concentration of ammonia vapor in air increases (Fig. 8). The polynomial fit for that with ammonia vapor concentration is shown in Fig. 8.

Ammonia vapor sensing characteristics

The doping of PmAP is not possible with HCl [36] due to presence of hydrogen bonding with the active –NH-site. Again, the only silver nanocomposite film (undoped one) shows very high resistivity ($10^{8\text{--}9}$ order) and thus ammonia-sensing study is also very difficult when using undoped PmAP–silver nanocomposite film. So, the ammonia vapor sensing behavior of hydrochloric acid doped PmAP–silver nanocomposite is studied and the plots are shown in the

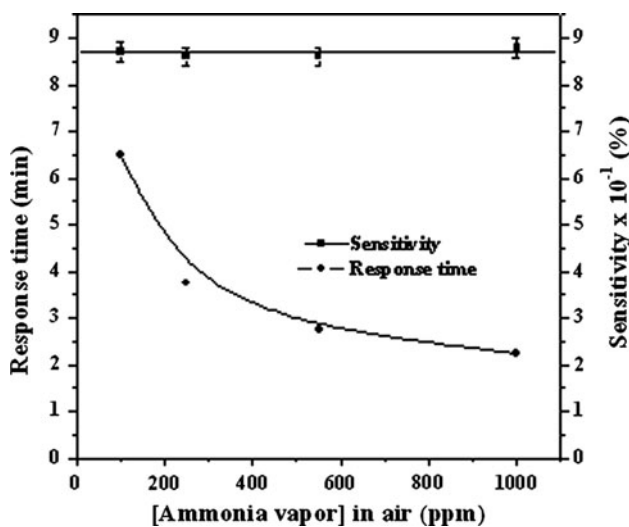


Fig. 8 Ammonia vapor sensing kinetics of HCl-doped PmAP–silver nanocomposite at varying concentration in air mixture

Table 2 Ammonia-sensing properties of HCl-doped PmAP–silver nanocomposite

[NH ₃] in air (ppm)	Response time (min)	Recovery time (min)	Sensitivity (%)
100	7.00	6.50	88
250	3.75	8.00	84
550	2.75	8.25	85
1,000	2.25	7.75	89

Figs. 7, 8, 9 and 10. The ammonia vapor sensing at varying concentrations in air results in decreasing the resistivity of nanocomposite films (Fig. 7). The mechanism responsible is well explained in the previous section. The average sensitivity is 86.75% with a standard deviation of ± 2.9 for the ammonia vapor sensing at varying concentrations of ammonia vapor in air by the doped nanocomposite film (Fig. 8). The results obtained using one sample for all the concentrations or different samples for different concentrations are similar (i.e., the sensitivity range is within the standard deviation value). Here, ammonia is a small molecule and can occupy almost all the –OH groups, which are made free by the silver nanocomposite. For that reason the composite shows constant response (Fig. 8; Table 2) with respect to the ammonia concentration. Only for the lower concentration, the response time is high and as the concentration of ammonia vapor in air increases to 1,000 from 100 ppm, the response time gradually decreases from 6.5 to 2 min (Table 2). This happens due to the availability of greater number of ammonia molecules to occupy more active sites (Scheme 1) in less time for higher ammonia vapor concentration. The recovery times are almost same for the sensing of all the ammonia vapor concentration and it is around 6–8 min (Table 2). For the reproducibility study the sensing characteristics of nanocomposite film up to consecutive six cycles are shown in Figs. 9 and 10 for 500 and 1,000 ppm ammonia vapors, respectively. From the figures (Figs. 9, 10), it is clear that the sensing of ammonia vapor by the doped film has very good reproducibility. The sensitivity range for consecutive cycles is within the standard deviation value.

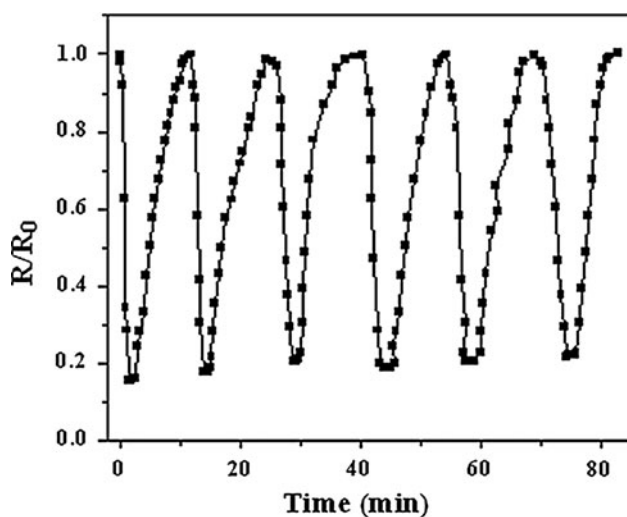


Fig. 9 Sensing reproducibility of HCl-doped PmAP–silver nanocomposite film on exposure to 500 ppm ammonia vapor-air mixture

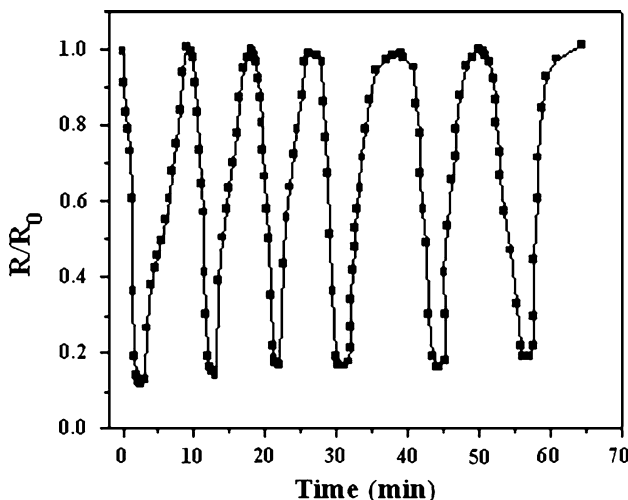


Fig. 10 Sensing reproducibility of HCl-doped PmAP–silver nanocomposite film on exposure to 1,000 ppm ammonia vapor–air mixture

Conclusion

In the continuous flow of air ammonia vapor mixture, the hydrochloric acid doped PmAP–silver nanocomposite gives good response by altering the resistivity at room temperature and room humidity. The doped nanocomposite also shows good response and recovery times for ammonia vapor. The average sensitivity is very good ($86.75 \pm 2.9\%$) and it does not vary with varying concentration of ammonia in air, although the response time varies with varying concentration of ammonia vapor. Again the reproducibility for the sensing of ammonia vapor is quite good. So, we can conclude that hydrochloric acid doped PmAP–silver nanocomposite can be used as a very good sensing material to fabricate ammonia-sensing devices. This is because unlike other nanocomposites such as carbon nanotubes or other metal nanocomposites here the sensitivity does not depend on the ammonia concentration.

References

- Adhikari B, Majumdar S (2004) Prog Polym Sci 29:699
- Saxena V, Malhotra BD (2003) Curr Appl Phys 3:293
- Ma X, Li G, Wang M, Chen H (2006) J Mater Sci 41:7604. doi:[10.1007/s10853-006-0849-2](https://doi.org/10.1007/s10853-006-0849-2)
- Li W, Kim D (2010) J Mater Sci. doi:[10.1007/s10853-010-5013-3](https://doi.org/10.1007/s10853-010-5013-3)
- Firth AV, Haggata SW, Khanna PK, Williams SJ, Allen JW, Magennis SW, Samuel IDW, Cole-Hamilton DJ (2004) J Lumin 109:163
- Chang Q, Zhao K, Chen X, Li M, Liu J (2008) J Mater Sci 43: 5861. doi:[10.1007/s10853-008-2827-3](https://doi.org/10.1007/s10853-008-2827-3)
- Windlass H, Raj PM, Balaraman D, Bhattacharya SK, Tummala RR (2003) IEEE Trans Adv Packag 26:10
- Bai Y, Chen ZY, Bharti V, Xu HS, Zhang QM (2000) Appl Phys Lett 76:3804
- Saujanya C, Radhakrishnan S (2001) Polymer 42:6723
- Nogales A, Broza G, Roslaniec Z, Schulte K, Sics I, Hsiao BS, Sanz A, Garcia-Gutierrez MC, Rueda DR, Domingo C, Ezquerro TA (2004) Macromolecules 37:7669
- Hanglein A (1989) Chem Rev 89:1861
- Shipway AN, Katz E, Willer I (2000) Chem Phys Chem 1:18
- Ng K, Montly G, Li Y, Yaniv Z, Soundarajan P (2004) US Patent 2,004,261,500, 2004, p 23
- Haes AJ, Duyne RPV (2002) J Am Chem Soc 124:10596
- Erisman JW, Otjes R, Hensen A, Jongejan P, Bulk PVD, Khlystov A, Mols H, Slanina S (2001) Atmos Environ 35:1913
- Dhawan SK, Kumar D, Ram MK, Chandra S, Trivedi DC (1997) Sens Actuators B: Chem 40:99
- Debarnot DN, Epaillard FP (2003) Anal Chim Acta 475:1
- Koul S, Chandra R, Dhawan SK (2001) Sens Actuators B: Chem 75:151
- Chabukswar VV, Pethkar S, Athawale AA (2001) Sens Actuators B: Chem 77:657
- Deng A, Cheng J, Huang H (2002) Anal Chim Acta 461:49
- Huang J, Virji S, Weiller BH, Kaner B (2003) J Am Chem Soc 125:314
- Sengupta PP, Kar P, Adhikari B (2009) Thin Solid Films 517: 3770
- Kukla AL, Shirshov YM, Piletsky SA (1996) Sens Actuators B: Chem 37:135
- Athawale AA, Chabukswar VV (2001) J Appl Polym Sci 79:1994
- Krutovertsov SA, Sorokin SI, Zorin AV, Letuchy YA, Antonova OY (1992) Sens Actuators B: Chem 7:492
- Sing FY, Hui SS, Rong ZD (2000) Talanta 51:151
- Kar P, Pradhan NC, Adhikari B (2008) Mater Chem Phys 111:59
- Schroder DK (1990) Semiconductor material and device characterization. John Wiley & Sons, New York, p 2
- Sengupta PP, Barik S, Adhikari B (2006) Mater Manuf Proc 21:263
- Tan CK, Blackwood DJ (2000) Sens Actuators B: Chem 71:184
- Kar P, Pradhan NC, Adhikari B (2009) Sens Actuators B: Chem 140:525
- Genies EM, Boyle A, Lapkowski M, Tsintavis C (1990) Synth Met 36:139
- Kulkarni VG, Campbell LD, Mathew WR (1989) Synth Met 30:321
- Wang XH, Geng YH, Wang LX, Jing XB, Wang FS (1995) Synth Met 69:265
- Lux F (1994) Polymer 35:2915
- Kar P, Pradhan NC, Adhikari B (2008) J Polym Mater 25:387
- Kar P, Pradhan NC, Adhikari B (2009) Polym Adv Technol. doi:[10.1002/pat.1622](https://doi.org/10.1002/pat.1622)
- Rivas BL, Sanchez CO, Berndt CJ, Mollinie P (2002) Polym Bull 49:257
- de Oliveira ZT Jr, dos Santos MC (2000) Chem Phys 260:95
- Zhang Z, Zhang L, Wang S, Chen W, Lei Y (2001) Polymer 42: 8315
- Lu X, Huang D, Yang X, Huang W (2006) Polym Bull 56:171
- Dimitriev OP (2003) Polym Bull 50:83
- Choudhury A (2009) Sens Actuators B: Chem 138:318